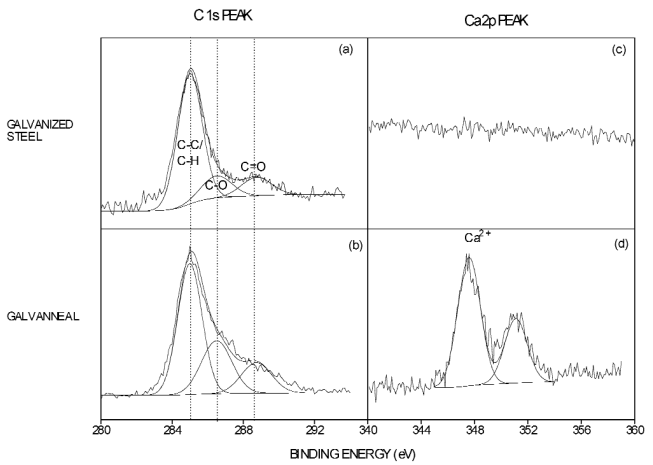

Fig. 4—C1s and Ca2p high-resolution XPS spectra obtained on the surface of pure Zn and galvanneal coatings.

on the outer surface of the coating obtained by hot galvanization, in which the Fe-Zn alloy forms only a thin layer close to the steel surface followed by a zinc layer of much greater thickness (schematic picture in Figure 3(c)). In the case of the galvanneal coating, the growth of the Fe-Zn alloy would push the contamination toward the outer surface of the coating (Figure 3(d)), while on the galvanized coating, it would remain at the Fe-Zn alloy/Zn interface (Figure 3(d)), and thus be impossible to detect. This phenomenon is somewhat similar to other cases reported in the literature, *e.g.*,

1. that iron oxide films present on the steel surface are ejected during galvanization into the zinc melt,
2. that these films are incorporated in the Fe-Zn alloy/Zn interface,[13] and
3. that in Zn(Al) baths, the Fe_2Al_5 inhibiting layer is pushed into the melt during the formation of the galvanized coating.[14]

The authors acknowledge the European support of this research (ECSC Projects Nos. 7210-PR-119 and 7210-PR-121).

REFERENCES

1. I. Hertveldt, B.C. De Cooman, and S. Claessens: *Metall. Mater. Trans. A*, 2000, vol. 31A, pp. 1225-32.
2. A.R. Marder: *Progr. Mater. Sci*., 2000, vol. 45, pp. 191-271.
3. S. Feliu, Jr. and M.L. Pérez-Revenga: *Metall. Mater. Trans. A*, 2004, vol. 35A, pp. 0000-00.
4. A. Henion: ECSC Project No. 7210-PR/119, Final Report, ECSC, Luxembourg, 2002.
5. G. Kurbatov, E. Darque-Ceretti, and M. Aucoutier: *Surf. Interface Anal*., 1993, vol. 20, pp. 402-06.
6. D.R. Cousens, B.J. Wood, J.Q. Wang, and A. Atrens: *Surf. Interface Anal*., 2000, vol. 29, pp. 23-32.
7. Th. Mayer: *Appl. Surf. Sci.*, 2001, vol. 179, p. 257.
8. U. Clofsson and S. Didzar: *Wear*, 1998, vol. 215, p. 156.
9. E.J. Ekanem, J.A. Lori, and S.A. Thomas: *Talanta*, 1997, vol. 44, p. 2103.
10. P.E. Lafargue, N. Chaoui, E. Millon, J.F. Muller, H. Derule, and A. Popandenec: *Surf. Coating Technol.*, 1998, vol. 106, p. 268.
11. P. Gouérec, M. Savy, and J. Riga: *Electrochim. Acta.*, 1998, vol. 43, p. 743.
12. B. Chatelain and V. Leroy: *La Rev. Metall. CIT*, 1998, vol. 6, p. 331.
13. C.E. Jordan and A.R. Marder: *Metal. Mater. Trans. B*, 1998, vol. 29B, pp. 479-84.
14. M. Guttmann: *Mater. Sci. Forum*, 1994, vols. 155–156, p. 527.

The Dependence of Cavity-Growth Rate on Stress Triaxiality

P.D. NICOLAOU, S.L. SEMIATIN, and A.K. GHOSH

The hot working of metals is often accompanied by the formation of internal cavities. The cavitation process can be divided into three distinct, but usually overlapping, stages—nucleation, growth, and coalescence. Moreover, the extent of cavitation (*e.g.*, cavity size and volume fraction) often exhibits a strong dependence on alloy composition and microstructure as well as on the imposed processing conditions (temperature, strain, strain rate, stress state). The development of an understanding of cavitation is important because it may limit hot workability as well as have a deleterious effect on final service properties.[1–4]

The uniaxial tension test has been frequently used to study cavitation in a number of materials including alloys of titanium, aluminum, copper, lead, and iron. Such tests enable the determination of important damage parameters such as cavity-nucleation strain, cavity-nucleation rate, and cavity-growth rate as well as those processing conditions under which cavitation is more or less severe. Although uniaxial-tension tests are relatively simple to perform, the results from such experiments are generally limited to the specific stress state characterizing these tests. However, cavity growth is known to depend markedly on the stress state and in particular on the ratio of mean-to-effective stress (σ_M/σ_e). Given the importance of cavitation during bulk hot working (*e.g.*, forging) and superplastic sheet forming, a quantitative relation describing the dependence of the cavity-growth rate on stress state would be very useful. To this end, extensive theoretical research has been conducted to develop models of cavity growth. In additional, physical modeling has been conducted to simulate cavitation behavior under complex stress states; the majority of this work has employed simulative workability techniques such as the notched-tension test[5,6] and biaxial and plane-strain testing.[7]

The objective of the current work was to establish a correlation between the cavity-growth rate and stress state by comparing the predictions of different theoretical and phenomenological models with each other as well as with experimental results from several prior efforts reported in the literature. With such a correlation, observations from simple tension tests can then be used to predict cavitation characteristics under conditions characterized by complex stress states.

Cavity growth models. For plasticity-controlled growth, the relation that describes cavity growth is usually of the following form:

$$r = r_0 \exp\left[(\eta^{ts}/3)\,(\varepsilon - \varepsilon_{\text{nucl}})\right] \qquad [1]$$

in which r_0 denotes the initial cavity radius, ε is the true strain, $\varepsilon_{\text{nucl}}$ is the cavity-nucleation strain, and η^{ts} is the cavity-

P.D. NICOLAOU, R&D Scientist, is with S&B S.A., 106 72 Athens, Greece. Contact e-mail: p.nicolaou@s.andb.gr S.L. SEMIATIN, Senior Scientist, Materials/Processing/Processing Science, is with the Air Force Research Laboratory, Materials and Manufacturing Directorate, AFRL/MLLM, Wright-Patterson Air Force Base, OH 45433-7817. A.K. GHOSH, Professor, is with the Department of Materials Science and Engineering, University of Michigan, Ann Arbor, MI 48109-2136.

Manuscript submitted December 9, 2003.

growth rate for an arbitrary stress ratio σ_M/σ_e. The nucleation strain ε_{nucl} is the strain at which cavities can be detected by optical microscopy, *i.e.*, they have a size of about 1 μm. Equation [1] describes the growth of larger cavity sizes, *i.e.*, over 1 μm. On the other hand, for smaller, submicron cavity sizes, the interface-constrained plasticity model by Ghosh *et al.*,[8] reveals that such cavities grow at much higher rates because of high local hydrostatic stresses arising from plastic constraints. The increase of the cavity-growth parameter due to stress triaxiality is proportional to a function of the ratio of mean stress σ_M to effective stress σ_e, $F(\sigma_M/\sigma_e)$; *i.e.*,

$$\eta^{ts} = \eta F(\sigma_M/\sigma_e) \qquad [2]$$

in which η denotes the cavity-growth parameter under uniaxial-tension conditions.

Combining Eqs. [1] and [2], the following general relationship is thus derived:

$$r = r_0 \exp\left[\frac{\eta}{3} F\left(\frac{\sigma_M}{\sigma_e}\right)(\varepsilon - \varepsilon_{nucl})\right] \qquad [3]$$

The function $F(\sigma_M/\sigma_e)$ has been determined by Rice and Tracey,[9] Thomason,[10] McClintock,[11] and Pilling and Ridley[12] using theoretical and experimental approaches. Rice and Tracey (RT)[9] considered a spherical void (cavity) within a plastic, nonhardening, Mises material. The strain field was determined from three contributions: (1) a uniform strain field due to plastic deformation of the matrix; (2) a spherically-symmetric strain field resulting from the change of the void volume but no shape change; and (3) a strain field (decaying at remote distances), which arises from changes of the void shape but not its volume. The theoretical analysis of RT revealed that the contribution of the change of the cavity shape in the strain field is minimal; on the other hand, the other two factors had a much more potent effect. The RT model was modified by Thomason[10] in order to take into account the change of size and shape of the initially spherical void. Thomason's model, which includes unilateral contact constraint, differs from that of RT in that it predicts a positive plastic dilatational strain under a pure deviatoric stress state, while the original RT model predicts no damage under these conditions. McClintock[11] proposed another model, which predicts the growth of an elliptical hole in a viscous material under an applied stress, assuming an axisymmetric geometry.

Pilling and Ridley[12] conducted experimental investigations to delineate the effect of the hydrostatic pressure on the cavity-growth rate for two superplastic alloys that exhibited extensive cavitation. Their work led to the following *empirical* relationship for the variation of the cavity-growth rate with stress triaxiality:

$$\eta^{ts} = \eta\left(1/3 + 2\frac{\sigma_M}{\bar{\sigma}}\right) \qquad [4]$$

Comparison of models and experimental data. To obtain a correlation between the cavity-growth rate and stress state, a number of prior experimental observations[5–7,13–15] were collected and analyzed. The data corresponded to a wide range of materials (*e.g.*, titanium alloys, aluminum alloys, steels, *etc.*) deformed under different applied stress states (*e.g.*, equibiaxial tension, plane strain tension, uniaxial tension of notched specimens, *etc.*) and processing conditions (*i.e.*, temperature, strain rate). From these prior measurements, a plot of the ratio of the cavity-growth rate under triaxial and uniaxial stress conditions (η^{ts}/η) as a function of the stress-triaxiality ratio (σ_M/σ_e) was made (Figure 1(a)). The increase in cavitation with stress triaxiality, as depicted in Figure 1(a), contains some scatter, the bounds of which are indicated by the shaded region. The scatter band encompasses all but a few of the experimental data points. Figure 1(a) also indicates a best-fit line through the data.

The experimental-data scatter band was compared to trend lines from the various models summarized previously (Figure 1(b)). The comparison showed that none of the models provide precise predictions of the experimental trends. Nevertheless, the semiempirical model of Pilling and Ridley (PR) mirrors the observed trend better than the other models. In fact, the upper and lower limits of the experimental scatter band follow the PR trend (Eq. [4]) when the latter is modified to include a factor Q, viz.:

$$\frac{\eta^{ts}}{\eta} = Q\left(1/3 + 2\frac{\sigma_M}{\sigma_e}\right) \qquad [5]$$

Specifically, the experimental observations are bounded by Eq. [5] using values of Q equal to 0.75 (lower bound) and 1.25 (upper bound).

Combining Eqs. [3] and [5], the general correlation of cavity growth and stress state can be described by the following relationship:

$$r = r_0 \exp\left[\frac{\eta}{3} Q\left(1.3 + 2\frac{\sigma_M}{\sigma_e}\right)(\varepsilon - \varepsilon_{nucl})\right] \qquad [6]$$

Application. The efficacy of the correlation described by Eqs. [5] and [6] was confirmed using two different sets of cavity-size measurements. The first set came from experiments involving a range of stress triaxialities developed during notched-tension testing of a titanium alloy,[5] while the second focused on results from the equibiaxial-tension testing of an aluminum alloy.[7]

Measurements of the average diameter of cavities developed during notched-tension testing of Ti-6Al-4V (with a colony-alpha microstructure) at 815 °C and a nominal strain rate of 0.1 s^{-1}[5] are plotted as a function of the stress triaxiality ratio σ_M/σ_e in Figure 2. The individual data points correspond to two different cavity-growth strain ranges, $\varepsilon - \varepsilon_{nucl}$. For the circular points, this strain range was between 0.10 and 0.16, and for the square data points, it was between 0.19 and 0.25. In addition, predictions for $\eta = 6.5$,[13] values of the constant Q between 0.75 and 1.25, and the same levels of $\varepsilon - \varepsilon_{nucl}$ (*i.e.*, ~0.14 and ~0.22) are also shown in the graph as shaded areas. It can be seen that the correlation of Eq. [6] bounds the experimental measurements fairly well.

Measurements (data points) of the effective-strain dependence of the average diameter of cavities developed during the equibiaxial-tension testing ($\sigma_M/\sigma_e = 0.66$) of a fine-grained, modified 5083 aluminum alloy containing Al-Mg-Mn at two different strain rates[7] and a temperature in the superplastic range are shown in Figure 3. Applying Eq. [6] for $Q = 0.75$

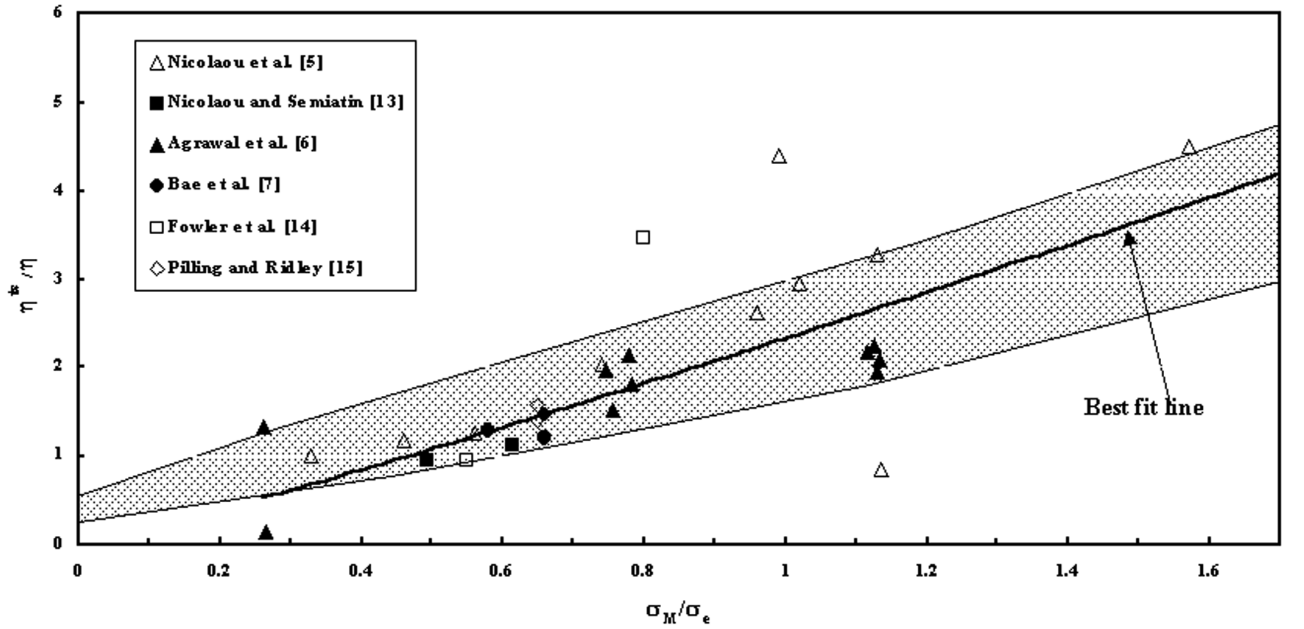

(*a*)

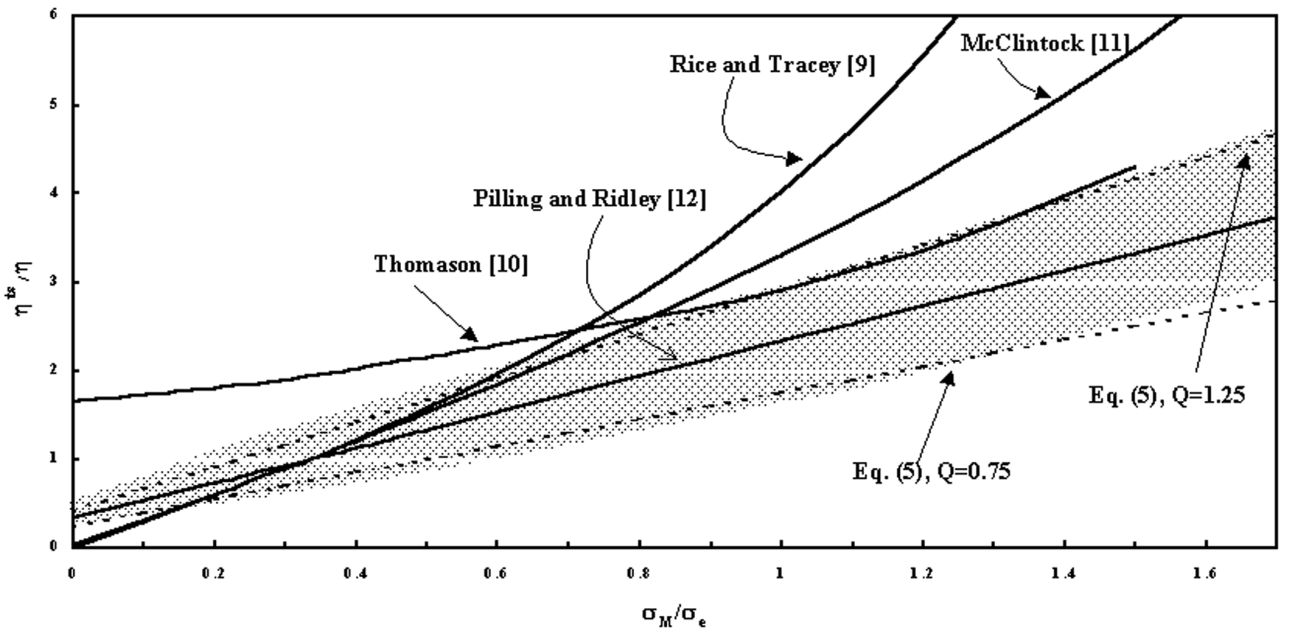

(*b*)

Fig. 1—Dependence of the ratio of the cavity-growth parameter under triaxial and uniaxial states of stress (η^*/η) on the stress triaxiality (σ_M/σ_e): (*a*) measurements from the literature and (*b*) comparison of the scatter band from (a) with various model predictions.

and 1.25, a cavity-growth rate in uniaxial tension of $\eta = 3.2$,[7] and an assumed nucleation strain of zero (solid lines), it is seen that this range of Q values bounds the observed data in this case also, consistent with the earlier finding.

In summary, a broad correlation between the growth rate of cavities developed during primary and secondary hot working and the stress triaxiality was deduced. The trends predicted by this correlation mirrored additional observations obtained during notched-tension testing of a titanium alloy and equibiaxial tension of an aluminum alloy. The upper bound of the correlation ($Q = 1.25$) can be used as a process design criterion in industrial applications.

This work was conducted as part of the in-house research activities of the Metals Processing Group of the Air Force Research Laboratory, Materials and Manufacturing Directorate. One of the authors (PDN) was supported under the auspices of Air Force Contract No. F33615-00-C-5212.

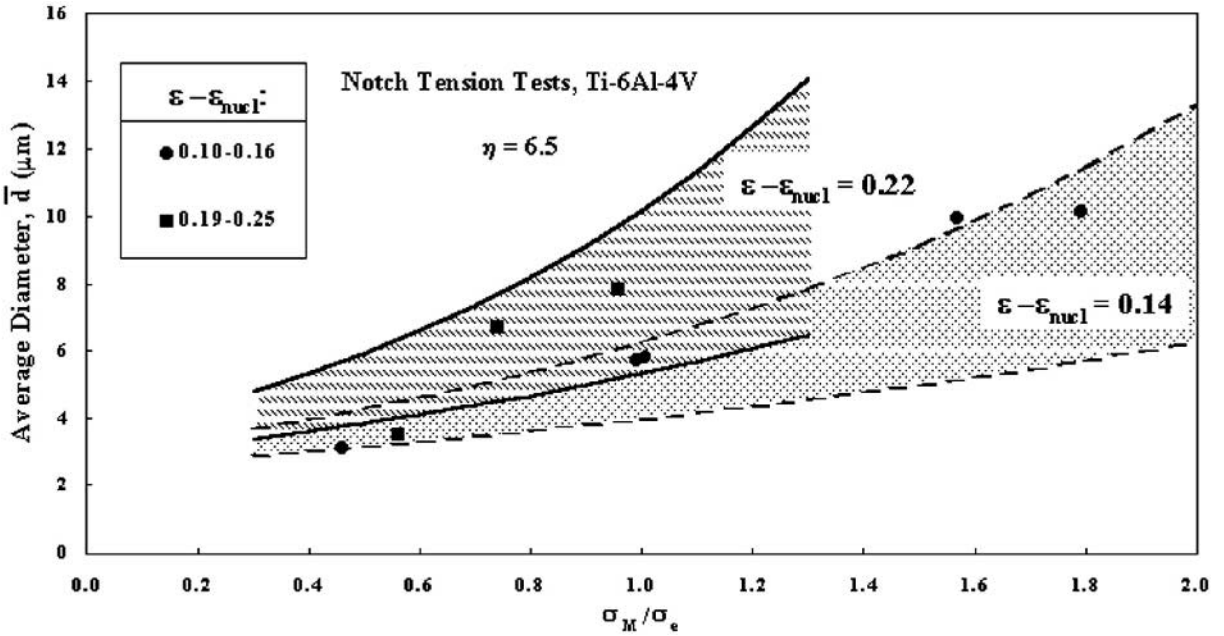

Fig. 2—Comparison of cavity sizes developed during notched-tension testing of Ti-6Al-4V as a function of stress triaxiality (data points) with the trends derived from Eq. [6] (shaded bands).

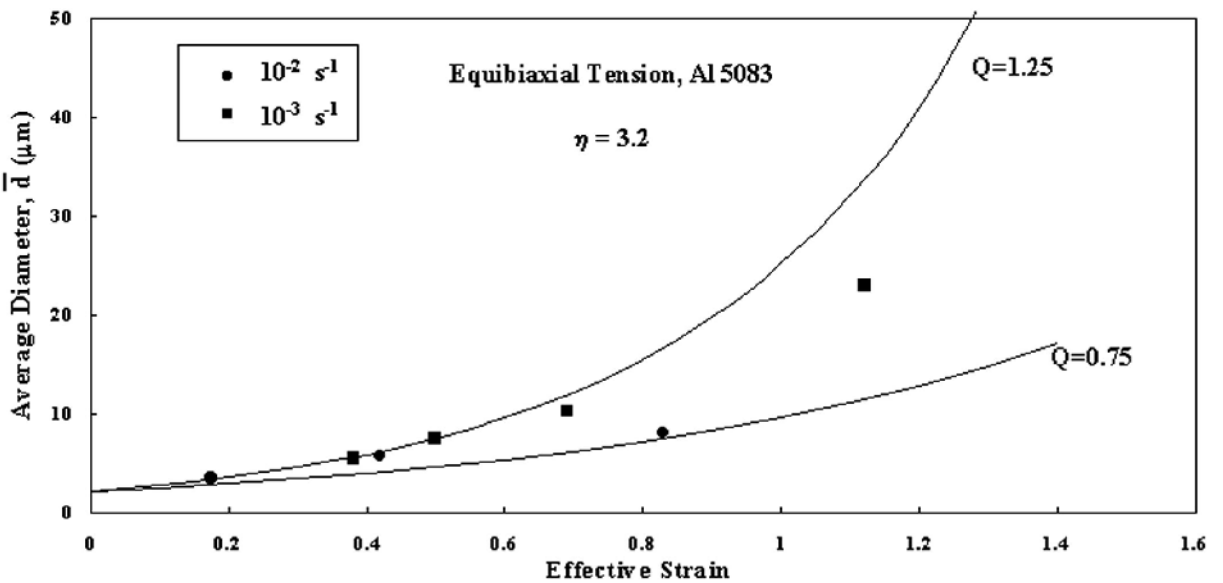

Fig. 3—Comparison of cavity sizes developed during equibiaxial-tension testing of a fine-grained 5083 modified aluminum alloy as a function of effective strain (data points) with the trends derived from Eq. [6] (lines).

REFERENCES

1. C.C. Bampton and J.W. Edington: *J. Eng. Mater. Technol.*, 1983, vol. 105, pp. 55-60.
2. R. Verma, P.A. Friedman, A.K. Ghosh, S. Kim, and C. Kim: *Metall. Mater. Trans. A*, 1996, vol. 27A, pp. 1889-98.
3. P.D. Nicolaou and S.L. Semiatin: *J. Mater. Sci.*, 2001, vol. 36, pp. 5155-59.
4. S.L. Semiatin, V. Seetharaman, A.K. Ghosh, E.B. Shell, M.P. Simon, and P.N. Fagin: *Mater. Sci. Eng. A*, 1998, vol. A256, pp. 92-110.
5. P.D. Nicolaou, R.L. Goetz, and S.L. Semiatin: *Metall. Mater. Trans. A*, 2004, vol. 35A, pp. 655-63.
6. H. Agarwal, A.M. Gokhale, S. Graham, and M.F. Horstemeyer: *Mater. Sci. Eng. A*, 2003, vol. A341, pp. 35-42.
7. D.H. Bae, A.K. Ghosh, and J.R. Bradley: *Metall. Mater. Trans. A*, 2003, vol. 34A, pp. 2449-63.
8. A.K. Ghosh, D-H. Bae, and S.L. Semiatin: *Mater. Sci. Forum*, 1999, vols. 304–306, pp. 609-16
9. J.R. Rice and D.M. Tracey: *J. Mech. Phys. Solids*, 1969, vol. 17, pp. 201-17.
10. P.F. Thomason: *Ductile Fracture of Metals*, Pergamon Press, New York, NY, 1990.
11. F.A. McClintock: *Trans. ASME, J. Appl. Mech.*, 1968, vol. 35, pp. 363-71.
12. J. Pilling and N. Ridley: *Acta Metall.*, 1986, vol. 34, pp. 669-79.
13. P.D. Nicolaou and S.L. Semiatin: *Acta Mater.*, 2003, vol. 51, pp. 613-23.
14. J.P. Fowler, M.J. Worswick, A.K. Pilkey, and H. Nahme: *Metall. Mater. Trans. A*, 2000, vol. 31A, pp. 831-44.
15. J. Pilling and N. Ridley: in *Superplasticity in Aerospace*, H.C. Heikkenen and T.R. McNelley, eds., TMS, Warrendale, PA, 1988, pp. 183-97.